Performance Constraints and Compensation For Teleoperation With Delay

J. S. McLaughlin
B. D. Staunton
The Aerospace Corporation
El Segundo, CA 90245

Abstract:

A classical control perspective is used to characterize performance constraints and evaluate compensation techniques for teleoperation with delay. Use of control concepts such as open and closed loop performance, stability, and bandwidth yield insight to the delay problem. Teleoperator performance constraints are viewed as an open loop time delay lag and as a delay-induced closed loop bandwidth constraint. These constraints are illustrated with a simple analytical tracking example which is corroborated by a real-time, man-in-the-loop tracking experiment. The experiment also provides insight to those controller characteristics which are unique to a human operator. Predictive displays and feedforward commands are shown to provide open loop compensation for delay lag. Low pass filtering of telemetry or feedback signals is interpreted as closed loop compensation used to maintain a sufficiently low bandwidth for stability. A new closed loop compensation approach is proposed that uses a reactive (or force feedback) hand controller to restrict system bandwidth by impeding operator inputs.

I) INTRODUCTION

This paper illustrates teleoperation performance constraints caused by time delays and discusses delay compensation methods. Use of control concepts such as open and closed loop performance yields insight to the delay problem. Teleoperator performance constraints are viewed as an open loop time delay lag and as a delay-induced closed loop bandwidth limitation. The work is motivated by real-time ground control of spacecraft, including remote piloting, docking, refueling, and servicing with broader application to any system faced with delay-induced performance degradation.

A typical architecture for ground control of spacecraft operations is pictured in Figure 1. A satellite is to perform a mission such as docking or servicing and is controlled in real-time by operators at a ground console through a communications link. Time delays result from signal time-of-flight and queing and processing at each of the nodes. For Earth-orbiting satellites, the node delays are dominant. This problem is represented in the following by separating controller commands from the plant by an uplink delay and the plant measurements from the controller by a downlink delay (Figure 2).

Time delays affect teleoperator performance, ultimately destabilizing the system. The significance of these effects depends on the magnitude of the delay with respect to the bandwidth of the tasks involved. The emphasis of this paper is on the closed loop performance limitations caused by the delay. This paper offers a perspective from which to clarify performance issues and evaluate compensation approaches. System design considerations have also emerged from this perspective.

In Section II, classical control concepts are used to give a heuristic explanation of the performance degradation due to delay. An analytical example is introduced in Section III to quantify the stability constraint for a simple system. This effect is illustrated by a "stability boundary" in a plot of loop delay versus bandwidth showing the upper bound on closed loop bandwidth caused by the delay. A man-in-the-loop experiment is described in Section IV, whose results are consistent with the analytical findings. The experiment also provides insight to the controller characteristics of a human operator. Methods to compensate for delay-induced performance degradation are discussed in Section V. In particular, the utility of dynamic predictors, telemetry filtering, and predictive displays is addressed. In addition, a new closed loop compensation approach is proposed that uses a reactive (or force feedback) hand controller to restrict system bandwidth by impeding operator inputs.

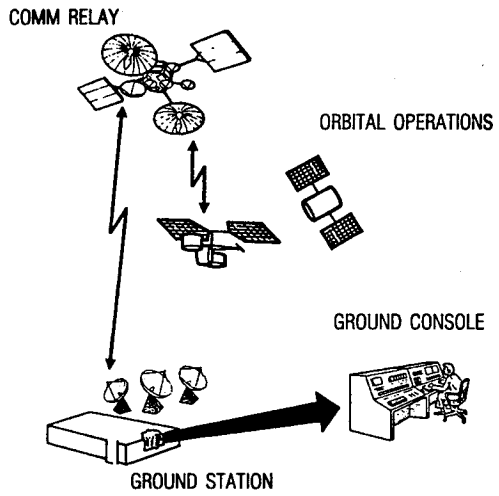

Figure 1: Ground Control of Spacecraft

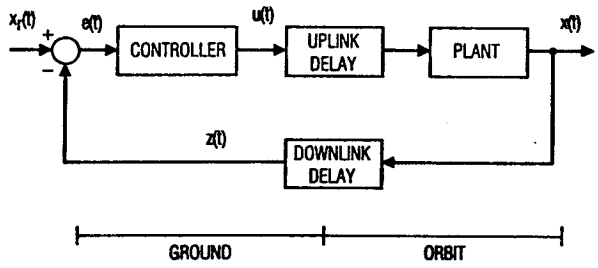

Figure 2: Idealized Block Diagram of Tracking with Delay

II) EFFECTS OF DELAY

The purpose of this section is to focus on a closed loop performance issue in teleoperation with delay and describe a way to characterize it. This is accomplished by making a distinction between open and closed loop control in teleoperation and providing intuitive explanations for the effects of time delay on each. From this, a bandwidth constraint is formulated and related to physical principles.

It has been useful in this work to consider open and closed loop commanding separately when investigating the effects of delay. An open loop command depends only on knowledge of the initial state (or measurement) of the system and is *independent* of the current measurement of the system. A closed loop command is generated from the current state through feedback, usually as corrections to errors from the desired state of the system.

In open loop control, models of the system and environment are used to compute open loop commands which drive the system in a desired fashion. An unmodeled delay introduces position errors resulting from lags in the system response. This can be corrected for by including the time delay in the model used to generate the commands. In addition, unmodeled disturbances introduce position errors. In fact, *all* errors from the desired path are a result of inaccuracies in the models used to generate the open loop commands. Open loop control cannot compensate for unknown characteristics of the system.

Closed loop control is used to improve tracking performance in the presence of model uncertainties and/or disturbances. A closed loop command is generated by a control law that operates on system errors determined by measurements of the state of the system. In the experiment described below, the control law is a human operator generating commands while watching a video display . Closed loop stability is intuitively related to error correction: if the errors are changing quickly relative to the delay, then using a relatively "old" measurement to make a correction is ineffective and could compound the errors (i. e., become unstable). The controller is only able to make stable corrections for errors that change slowly with respect to the loop delay. In other words, the bandwidth of the controller is limited. This in turn will limit overall system tracking or disturbance rejection performance.

This intuitive argument on the destabilizing effect of time delays can be related to the fundamental principle of the causality of physically realizable systems, which means that physically realizable systems cannot know the future. A closed loop controller that alleviates the bandwidth limitation will have some component that requires knowledge of a future state and therefore cannot be implemented. A controller that *predicts* the future state based on a model of the system and knowledge of the current state is an open loop controller and will not improve the closed loop bandwidth limitation.

III) STABILITY BOUNDARY: ANALYTICAL EXAMPLE

This section describes the procedure for arriving at quantitative delay-induced performance constraints in the form of a stability boundary. The effect of time delays is considered for deterministic, continuous, linear, time-invariant plants and full state feedback (FSFB), constant gain controllers. Time delays in the up and downlinks result in a transcendental characteristic equation which is solved and the dependency on total loop delay shown. The distribution of delays between the up and downlink segments are shown to have no effect on systems with this type of controller.

These systems can be represented in state space form as:

$$\dot{x}(t) = Ax(t) + Bu(t - T_u) \tag{1}$$

$$u(t) = -Kx(t - T_d) \tag{2}$$

where A is the plant dynamics matrix, B is the control distribution matrix, K is the feedback gain matrix, x is the state vector, and u is the control signal. Use of FSFB assumes that the entire state vector is available for control. $u(t-T_u)$ in equation (1) indicates that the plant dynamics are influenced by a control signal that has been delayed by T_u seconds in the uplink. $x(t-T_d)$ in equation (2) shows that the current control signal is computed from state measurements delayed by T_d seconds in the downlink.

Using Laplace transforms, these equations can be represented in the frequency domain as:

$$sx(s) = Ax(s) + Be^{-sT_u}u(s) \tag{3}$$

$$u(s) = -Ke^{-sT_d}x(s) \tag{4}$$

where s is the independent frequency parameter and e^{-sT} is the Laplace transform of a pure time delay of T seconds.

Some matrix algebra results in:

$$[sI - (A - BKe^{-s(T_u + T_d)})]x(s) = [0] \tag{5}$$

where I is the identity matrix, [0] is the zero matrix of appropriate dimensions, and multiplication of the exponential delay terms results in the sum of the delays in the exponent. Note that for the case of FSFB, only the *total* loop delay is significant, not the location of the respective delays.

In order for a non-zero solution of x(s) to exist, the coefficient matrix in equation (5) must be singular over all frequencies s. This can be stated by requiring the determinant of the matrix to be equal to zero:

$$\det[sI - (A - BKe^{-s(T_u + T_d)})] = 0 \tag{6}$$

Equation (6) is known as the characteristic equation for the feedback system represented in equations (1) and (2). Stability of the system is guaranteed if the real part of all roots of the characteristic equation are negative (Reference 1). Although the plant dynamics matrix A is finite dimensional, the system is infinite dimensional because of the time delay (as seen by Taylor series expansion of the exponential term in (6) which results in a polynomial in s with *infinitely* many terms). This complicates the solution of the characteristic equation and thus the determination of stability.

The characteristic equation for a simple second order system is solved here to illustrate delay-induced performance constraints. The system is representative of a positioning device with unit mass load and constant gain FSFB through a delay T. All stable roots of the characteristic equation are found (see Appendix) in order to compute an upper bound on system bandwidth as:

$$r < \frac{\cos^{-1}(\zeta)}{T\sqrt{1 - \zeta^2}} \quad , \quad \zeta \in (0, 1) \tag{7}$$

where ζ is a damping parameter that governs transient response behavior such as overshoot and settling time. The bandwidth is defined here as the magnitude r of the smallest root of the characteristic equation in (6). (The traditional definition of the -3 db crossover frequency in the closed loop transfer function differs slightly from that used in this paper depending on the damping of the fundamental response.)

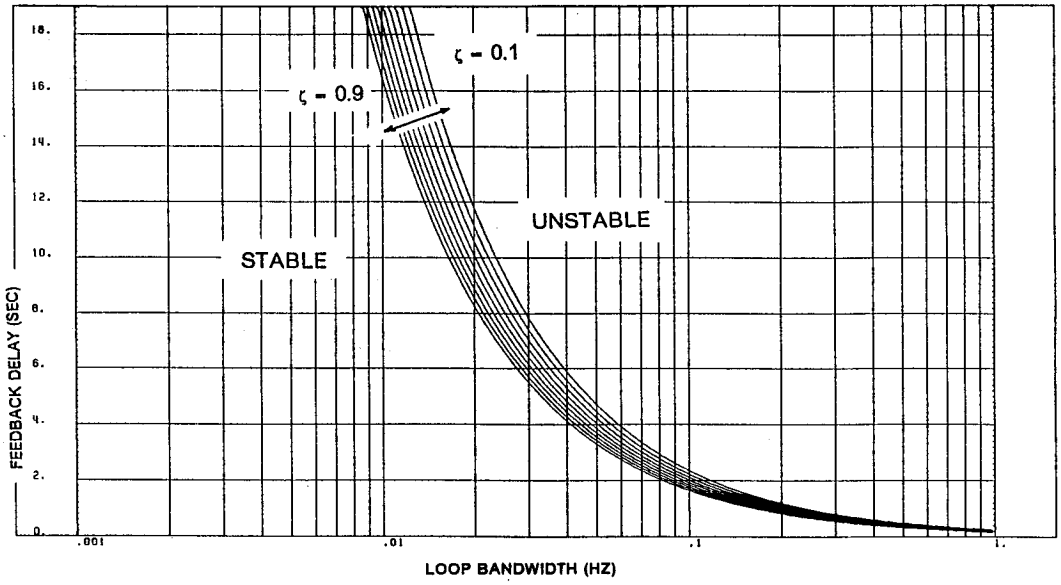

Figure 3: Stability Boundary for Second Order Example

Equation 7 is an inverse relationship between maximum system bandwidth and loop delay that is plotted in Figure 3 as a family of stability boundaries parameterized by ζ. For a given delay, controller parameters should be selected to ensure that the system bandwidth is low enough to fall within the stable region in Figure 3. Other criteria will influence the control design as well; this example serves to illustrate only the effects of time delay on closed loop performance.

IV) MAN-IN-THE-LOOP EXPERIMENT

A man-in-the-loop tracking experiment was conducted to test the closed loop stability boundary result of the analytical example. This section describes the experiment set-up and data gathering procedure, presents the significant results, and compares the findings to those from the analytical example.

The experiment involves the simulated motion of two vehicles, a graphic display of one (the target) as viewed from the second (the tracker), and a human operator. The operator sees the target from the perspective of the tracker. The operator inputs commands through a keyboard while watching the display which is driven by a real-time simulation of the tracking dynamics and delays. The total delay includes uplink and downlink delays, and an additional delay due to an inherent lag in the operator's response.

The target moves side-to-side in a one-dimensional motion perpendicular to the target/tracker line-of-sight. The target motion is oscillatory with random peak amplitudes and a frequency upper bound that is successively increased to find the stability boundary. Random amplitudes are used to prevent the operator from predicting the motion. Steps are taken to eliminate operator use of a fixed reference point (the zero crossing point of the target oscillatory motion).

The operator commands the tracking vehicle to follow the target while watching the relative vehicle positions in the display. Two keyboard keys are used to apply discrete velocity control in one dimension. To avoid corruption of the stability results, steps are taken to provide the operator with sufficient control authority for tracking all target motion frequencies.

The bandwidth constraint for this man-in-the-loop system is inferred from the maximum target frequency the operator is able to successfully track. The target motion frequency and uplink and downlink time delays are prescribed for each run which lasts 100 to 300 seconds, depending on the period of target motion. The data gathering procedure allows for a number of practice runs for each time delay/motion frequency case; the best run is saved. Position-time histories of both vehicles are recorded and plotted after each run.

Interpreting the tracking results in terms of stability can be difficult. Unlike an analytical controller, an experienced human operator does not go unstable in the classical sense. When faced with target motion too fast for the given time delays, the operator chooses to issue very few commands and waits for the target to return rather than chasing it (this is why it is important to eliminate the fixed reference point). The operator

learns to lower his bandwidth sufficiently for stable tracking, eventually resorting to a move and wait strategy. In this process, tracking is significantly degraded. The experiment results are therefore interpreted as one of three qualitative tracking assessments: "unsatisfactory" tracking is used when the operator ceases to follow the target (described above), "satisfactory" tracking is used to indicate good performance in the traditional sense (small error), and "marginal" tracking is applied to cases in between.

Figure 4 shows example position-time history plots of the target and three separate tracking runs. The maximum target frequency is 0.03 hertz frequency and the three runs have delays of 0, 2, and 4 seconds. Note that tracking performance gets worse as delays are increased. The three cases are interpreted as "satisfactory," "marginal," and "unsatisfactory" tracking.

Time delay/target frequency cases were attempted over the envelope defined by the analytical results. Figure 5 shows results in terms of "unsatisfactory," "marginal," and "satisfactory" tracking, overlayed on a plot of the stability boundary from the analytical example. The experiment results are consistent with the analytical example: the teleoperator is unable to track outside the stable region. The three cases from Figure 4 are denoted in Figure 5 by triangles.

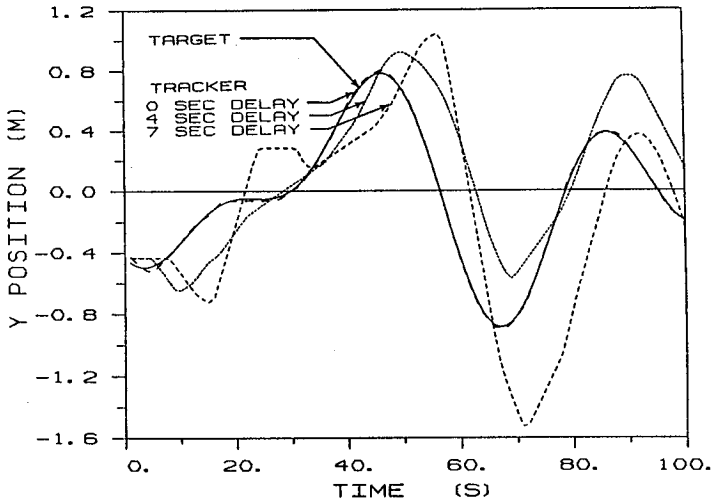

Figure 4: Man-in-the-Loop Tracking With Delay

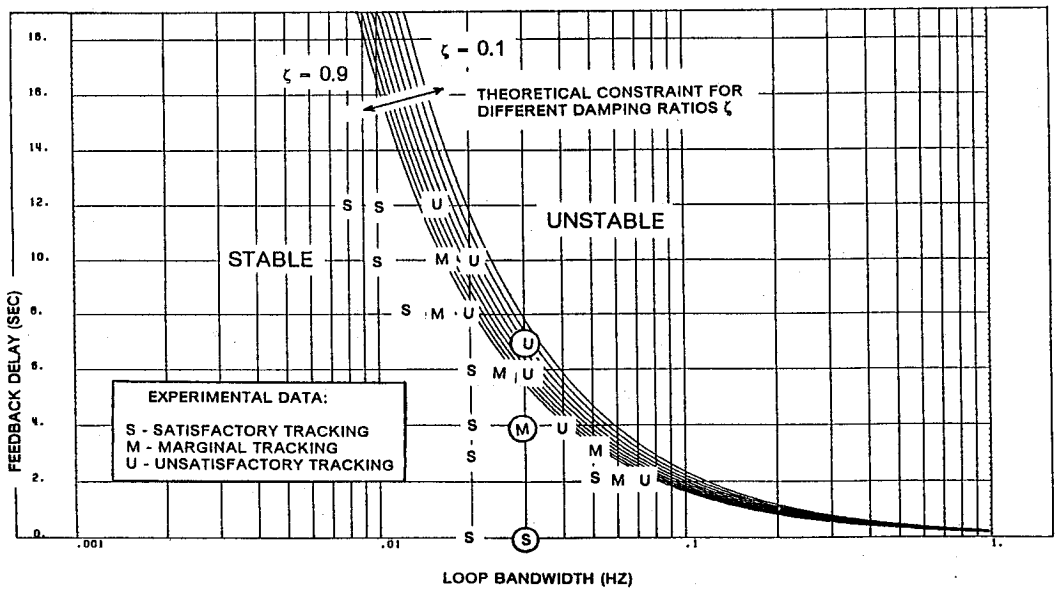

Figure 5: Stability Boundary With Man-in-the-Loop

V) DELAY COMPENSATION

The purpose of this section is to discuss delay compensation schemes that alleviate the performance degradation described above. Delay compensation approaches are described while maintaining the distinction between open and closed loop that has been useful in characterizing performance constraints. The goal of closed loop compensation is to maintain a stable closed loop bandwidth as close to the stability boundary as prudent while the aim of open loop compensation is to speed up the large motion segments of a task.

Closed Loop Compensation

A bandwidth constraint means that closed loop compensation must ensure the system bandwidth is maintained in the stable region and as close to the boundary as prudent to maximize performance. One way of limiting bandwidth is to use some sort of low-pass filtering on the up or downlink telemetry.

An idea introduced here is to use an active hand controller to lower the system bandwidth by impeding operator inputs. This effectively lowpass filters operator commands with enough impedance to ensure stability given the time delay. It is anticipated that the operator would not "fight" the stick to try and overcome the resistance but rather "feel" the effect of the time delay through the responsiveness of the stick and modulate his inputs accordingly. The desired result is to replace a move-and-wait strategy with slow, smooth commands generated from what is essentially a continuous "display" of time delay information (through stick impedance). The authors are considering experiments using hardware much like that used in force-reflecting hand controllers to investigate this form of delay compensation.

An alternative to impeding operator inputs is to display time delay information graphically. Experience with the man-in-the-loop tracking experiment suggests that knowledge of the time delay is beneficial. When motions are large, the delay is easily perceived from the lag between command and response. A graphical display of the time delay would provide the operator with delay information even when motions are small.

An additional consideration is that delays in a communications loop can change with time. In the tracking experiments, the operator appeared to be able to learn the (constant) delay over several trials with a marked improvement in performance. A delay that changes with time is likely to impede this learning, possibly with the operator retreating to some upper bound on the time delay variation.

The telemetry filter lowpass bandwidth and the hand controller impedance can be functions of the current time delay, known through time-tagged telemetry. This enables closed loop performance to be maximized even in the presence of time variable delays.

Open Loop Compensation

Although closed loop performance is limited by the bandwidth constraint, performance gains can be had with open loop (or feedforward) compensation in large motion segments of a task. Most manipulation tasks can be broken into large and small motion segments such as the slew and grapple segments in pick and place tasks. Here, fine position control is usually required only during the small motion segments where the manipulator has to be precisely positioned to grapple or place an object. During the large motion segments, position control requirements are relaxed and other performance objectives such as smoothness (to avoid disturbances) and minimum time are important.

Open loop compensation can be used to produce smooth and fast commands in these instances where exact position control is not required and a move-and-wait strategy is inefficient. This compensation requires models of the system and environment as well as knowledge of initial conditions to generate the commands.

A popular idea for delay compensation is to use predicted values of the current state in the control law instead of the delayed measurements.

Consider the plant equation (1) with no uplink delay and an additional input disturbance term f(t):

$$\dot{x}(t) = Ax(t) + Bu(t) + f(t) \tag{8}$$

Use a FSFB, constant gain controller operating on a predicted value of the state $\tilde{x}(t)$:

$$u(t) = -K\tilde{x}(t) \tag{9}$$

The state prediction $\tilde{x}(t)$ is generated by propagating ahead from a delayed state measurement x(t-T), including the effects of the control over the time interval (t-T,t):

$$\tilde{x}(t) = e^{AT}x(t - T) + \int_{t-T}^{t} e^{A(t-\tau)}Bu(\tau)d\tau \tag{10}$$

The prediction is actually the solution over the interval (t-T,t) of the differential equation in (8) without the disturbance f. The first term in (10) uses the state transition matrix to propagate the transient response over the interval and the second term propagates the forced response over that interval. For the purposes of showing the open loop behavior, this idealized predictor assumes exact plant knowledge, uncorrupted measurements and exact computation of the integral. Note that only the delayed state x(t-T) and the control history $\{u(\tau):\tau \in (t - T,t)\}$ are available to the predictor; the disturbance f(t) is unknown by definition.

Differentiate (10) to produce a differential equation for stability analysis:

$$\dot{\tilde{x}}(t) = e^{AT}[Ax(t - T) + Bu(t - T) + f(t - T)] + A[\tilde{x}(t) - e^{AT}x(t - T)] + Bu(t) - e^{AT}Bu(t - T) \quad (11)$$

where the plant dynamics (8) have been substituted for $\dot{x}(t - T)$ in the first term of (11), and (10) has been used to replace the integral left over after differentiation of the second term in (10).

Cancelling terms, noting that A and e^{AT} commute, gives:

$$\dot{\tilde{x}}(t) = A\tilde{x}(t) + Bu(t) + e^{AT}f(t - T) \quad (12)$$

Substitute (9) into (8) and (12), and combine into matrix form to get:

$$\frac{d}{dt}\begin{bmatrix} x(t) \\ \tilde{x}(t) \end{bmatrix} = \begin{bmatrix} A - BK & [0] \\ -BK & A \end{bmatrix}\begin{bmatrix} x(t) \\ \tilde{x}(t) \end{bmatrix} + \begin{bmatrix} [0] \\ [I] \end{bmatrix} f(t) + \begin{bmatrix} e^{AT} \\ [0] \end{bmatrix} f(t - T) \quad (13)$$

Note that the composite system dynamics matrix in (13) is triangular and that the open loop plant dynamics matrix A is on the diagonal, indicating that this form of compensation is open loop. Also note that disturbances affect the plant instantly, but have a delayed affect on the predictor since the predictor can only "see" the disturbance through the delayed state measurements. This predictor is an open loop command generator implemented by driving a "reference" model with the desired closed loop behavior. This scheme works best when the disturbance f is small relative to the control term Bu (e. g., during large motions), but cannot alleviate the closed loop bandwidth constraint.

In teleoperation, open loop compensation can be implemented with a predictive display which enables the operator to generate smooth, fast commands (References 2,3). The predictive display compensates for time delays by immediately displaying the results of the operator's commands, effectively creating a local, fast closed loop on the ground that generates a smooth, fast command sequence for the remote system (Figure 6). The loop is closed around an operator and a computer model of the manipulator and hence performance is determined by the quality of the model. The use of a predictive display has been demonstrated by Sheridan (Reference 3) to be effective in manipulator slewing applications. In this application, a predictive graphical overlay was used on a delayed video image of the manipulator.

It is possible that the predictor could be continuously updated by using an observer or estimator operating on the delayed feedback. However, these updates can only correct for slow, low bandwidth estimate errors because of the bandwidth constraint for the closed loop estimation process.

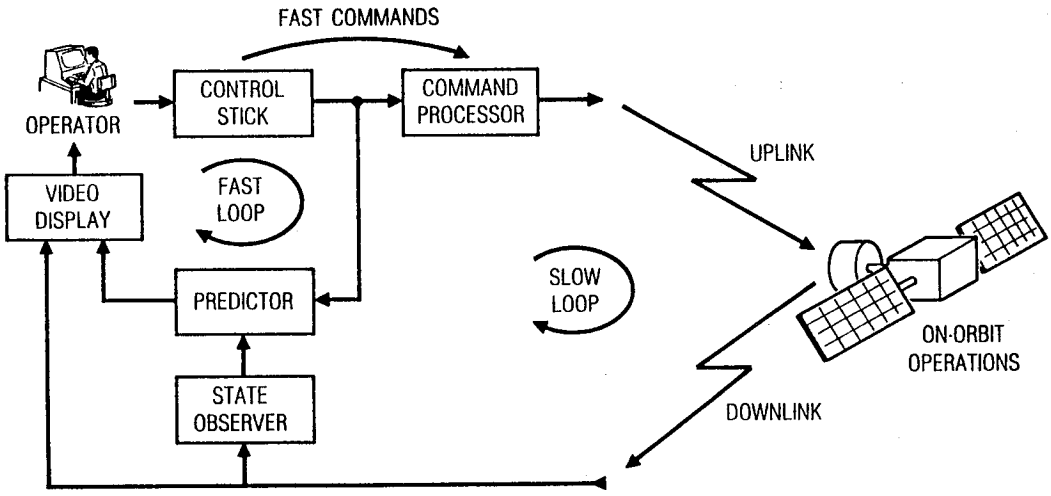

Figure 6: Predictive Display Block Diagram

VI) SUMMARY

The objective of this work is to characterize performance constraints and discuss compensation schemes in teleoperation with time delays. The distinction between open and closed loop in defining performance constraints and compensation schemes is essential. This distinction appears to be overlooked in current research which has motivated the present effort. An important performance constraint induced by delays is an upper bound on closed loop bandwidth. This constraint is related to the causality principle of physically realizable systems and and is illustrated with an example and man-in-the-loop experiment. This constraint is pictured as a stability boundary in plots of loop delay versus closed loop bandwidth. Open loop compensation is discussed as a way of improving large motion segments of a task, including the use of predictive displays in teleoperation. Closed loop compensation is described as maximizing bandwidth within the constraint imposed by time delays. A concept for the use of a resistive hand controller in delay compensation is introduced.

Top level conclusions can be drawn from the type of performance constraints described above. First, system architects must define requirements that reflect the delay-induced performance limitations in ground-based control of spacecraft. This realization influences the partitioning of tasks between those under direct ground control and those under local autonomous control. Telerobotics and hierarchical control concepts where a local computer assumes more of the control responsibilities could provide significant benefits here. Also, an emphasis on minimizing lags in communications systems would have a direct benefit in improving closed loop capabilities. A second conclusion concerns improving performance in the presence of delays. Proper use of both closed loop and open loop compensation schemes can maximize admissible bandwidth and speed up large motions.

A significant amount of work remains in this area. A more rigorous analytical definition of the bandwidth constraint and extension to higher order and more complex systems should be addressed. The relationship to man-in-the-loop needs further work, including investigations of man's inherent response lag and implementation of open and closed loop compensation.

ACKNOWLEDGEMENTS

This work was sponsored by W. I. Shanney of the Aerospace Corporation in support of the Air Force Satellite Control Network. The graphic display used in the experiment was developed by G. A. Irmen of The Aerospace Corporation.

REFERENCES

(1) Mori, T., et al.; "Analysis of Time Delay Systems: Stability and Instability", Proc. of 25th Conf. on Decision and Control, Dec. 1986, pp. 895-898.

(2) Conway, L., et al.; "Tele-Autonomous Systems: Methods and Architectures for Intermingling Autonomous and Telerobotic Technology", Proc. of IEEE Conf. on Robotics and Automation, 1987.

(3) Sheridan, T. B., et al; "MIT Research in Telerobotics", Proc. of the Workshop on Space Telerobotics, July 1987, Vol. 2, pp.403-412.

APPENDIX: SECOND ORDER SYSTEM

This example is of a positioning system driving a unit mass load with measurement delay of T seconds. The system matrices for equations (1) and (2) are:

$$A = \begin{bmatrix} 0 & 1 \\ 0 & 0 \end{bmatrix}, \quad B = \begin{bmatrix} 0 \\ 1 \end{bmatrix}, \quad K = [k_p \; k_d]$$

Where k_p and k_d are scalar proportional and derivative gains, respectively.

Plugging these values into (5) yields:

$$\begin{bmatrix} s & -1 \\ k_p e^{-sT} & s + k_d e^{-sT} \end{bmatrix} x(s) = [0] \qquad \text{(A1)}$$

The characteristic equation for this example is then:

$$e^{sT}s^2 + k_d s + k_p = 0 \qquad \text{(A2)}$$

Represent the complex variable s in polar coordinates:

$$s = re^{i\theta},\ r > 0,\ i = \sqrt{-1}, \tag{A3}$$

and use in (A2) to get:

$$e^{rTe^{i\theta}}r^2e^{2i\theta} + k_d re^{i\theta} + k_p = 0 \tag{A4}$$

Then use the identity:

$$e^{i\theta} = \cos(\theta) + i\sin(\theta) \tag{A5}$$

in (A4) and manipulate:

$$e^{rT(c\theta + is\theta)}r^2(c2\theta + is2\theta) + rk_d(c\theta + is\theta) + k_p = 0 \tag{A6}$$

$$\Rightarrow \quad e^{rTc\theta}[\cos(rTs\theta) + i\sin(rTs\theta)]r^2(c2\theta + is2\theta) + rk_d(c\theta + is\theta) + k_p = 0 \tag{A7}$$

The real part of (A7) is:

$$r^2e^{rTc\theta}[\cos(rTs\theta)c2\theta - \sin(rTs\theta)s2\theta] + rk_dc\theta + k_p = 0 \tag{A8}$$

and the imaginary part is:

$$r^2e^{rTc\theta}[\cos(rTs\theta)s2\theta + \sin(rTs\theta)c2\theta] + rk_ds\theta = 0 \tag{A9}$$

With some trig identities, these can be reduced to:

$$r^2e^{rTc\theta}\cos(rTs\theta + 2\theta) + rk_dc\theta + k_p = 0 \tag{A10}$$

$$r^2e^{rTc\theta}\sin(rTs\theta + 2\theta) + rk_ds\theta = 0 \tag{A11}$$

Combining (A10) and (A11) into a matrix equation yields:

$$\begin{bmatrix} 1 & rc\theta \\ 0 & rs\theta \end{bmatrix}\begin{bmatrix} k_p \\ k_d \end{bmatrix} = -r^2e^{rTc\theta}\begin{bmatrix} \cos(rTs\theta + 2\theta) \\ \sin(rTs\theta + 2\theta) \end{bmatrix} \tag{A12}$$

If $s\theta \neq 0$, then the coefficient matrix on the left hand side of (A12) can be inverted to solve for the controller gains:

$$\begin{bmatrix} k_p \\ k_d \end{bmatrix} = -\frac{r}{s\theta}e^{rTc\theta}\begin{bmatrix} rs\theta & -rc\theta \\ 0 & 1 \end{bmatrix}\begin{bmatrix} \cos(rTs\theta + 2\theta) \\ \sin(rTs\theta + 2\theta) \end{bmatrix}, \quad s\theta \neq 0 \tag{A13}$$

Multiplied out and using a trig identity, (A13) becomes:

$$\begin{bmatrix} k_p \\ k_d \end{bmatrix} = \frac{r}{s\theta}e^{rTc\theta}\begin{bmatrix} r\sin(rTs\theta + \theta) \\ -\sin(rTs\theta + 2\theta) \end{bmatrix} \tag{A14}$$

Stability requires the roots to be in the Left Half Plane (LHP) which restricts θ to $\theta \in (\frac{\pi}{2}, \frac{3\pi}{2})$. The fact that complex roots occur in conjugate pairs permits a further restriction of θ to the upper left quadrant:

$$\theta \in (\frac{\pi}{2}, \pi) \quad \Rightarrow \quad s\theta > 0 \tag{A15}$$

where only the first harmonic (smallest magnitude root) is considered.

Positive feedback gain $k_p > 0$ is assumed and (A15) is used to develop the following inequalities from (A14):

$$k_p > 0 \quad \Rightarrow \quad \sin(rTs\theta + \theta) > 0 \tag{A16}$$

$$\Rightarrow \quad (rTs\theta + \theta) \in (0, \pi) \tag{A17}$$

$$\Rightarrow \quad \theta < (\pi - rTs\theta) \tag{A18}$$

(A18) with (A15) gives:

$$\theta \in (\frac{\pi}{2}, \pi - rTs\theta) \tag{A19}$$

Now introduce the damping parameter ζ, related to θ by:

$$\cos(\theta) = -\zeta \quad \Rightarrow \quad \cos(\pi - \theta) = \zeta \tag{A20}$$

$$\sin(\theta) = \sqrt{1 - \zeta^2} \tag{A21}$$

Use (A20) and (A21) in (A18) and rearrange to get:

$$r < \frac{\cos^{-1}(\zeta)}{T\sqrt{1-\zeta^2}} \quad , \quad \zeta \in (0, 1) \tag{A22}$$

This is the bandwidth constraint for the second order example with the root magnitude r is constrained by an inverse function of delay. This is plotted in Figure 2 where the units of r have been changed from rad/sec to hz. Note that the boundary moves in as the damping parameter ζ is increased.